Optical characterization of a vertical cavity surface emitting laser for a coherent population trapping frequency reference

Christopher M. Long[a] and Kent D. Choquette[b]
Electrical and Computer Engineering Department, University of Illinois, Urbana, Illinois 61801, USA

(Received 14 June 2007; accepted 29 November 2007; published online 1 February 2008)

Characterization of a vertical cavity surface emitting laser source for a frequency reference that uses coherent population trapping with atomic rubidium is reported. The frequency reference requires a low-noise laser that operates in a single transverse mode at 794.7 nm. We show that biasing the laser at low output power and modulating it at higher frequency than its low relaxation oscillation frequency are necessary to obtain symmetric modulation sidebands and improve the long-term performance of the frequency reference. © *2008 American Institute of Physics*.
[DOI: 10.1063/1.2838175]

I. INTRODUCTION

Navigation and communication systems will benefit from compact frequency references that have greater accuracy. To meet this need, miniature, low-power frequency references with high precision and stability are under development.[1–3] One technique that is pursued is an atomic frequency reference based on the quantum mechanics phenomenon of coherent population trapping (CPT) because of its demonstrated stability and potential for size reduction in such a device.[4] In a CPT frequency reference, incident photons drive the electrons of an atom into a coherent dark state that prevents absorption from taking place. When this occurs, there is a detectable increase in transmitted power at a specific wavelength which is then used to create a frequency reference. Current research focuses on using a vertical cavity surface emitting laser (VCSEL) as the light source for the interrogation photons.[5] VCSELs are currently widely deployed as digital sources in data communication applications. A VCSEL is ideal for the frequency reference application because it consumes little power, experiences no optical mode hopping as it is tuned in frequency, and can be designed to emit photons in a single transverse mode.[6,7]

This study reports the optical characteristics of VCSELs designed for a CPT frequency reference that uses rubidium (Rb) vapor. Specific laser characteristics are studied that offer insight into the desired performance of VCSELs for this application. Section II presents the CPT approach in greater detail. Section III describes the VCSEL characterization including the spectral and modulation properties. Section IV analyzes the VCSEL frequency modulation, and we show that there is a significant advantage of biasing the VCSEL at low power and modulating it at higher frequency than its relaxation oscillation frequency, contrary to the usual operation of a data communications laser.

II. ATOMIC FREQUENCY REFERENCE

The frequency reference described herein[1] relies on atomic transitions between the $5S_{1/2}$ ground state and the $5P_{1/2}$ excited state of Rb, leading to the D_1 absorption line at a wavelength of 794.7 nm. When a magnetic field is applied to the atom, the Zeeman effect causes the energy states to separate into a manifold of sublevels; in the CPT process, we concentrate on the three specific sublevels shown in Fig. 1. The energy diagram in Fig. 1 shows two lower levels separated by the hyperfine frequency ν_{hf} of 6834 MHz and a single upper level. Shown also are two coherent optical light fields with frequencies ω_1 and ω_2. A photon at either of these frequencies could be absorbed by the atom and drive an electron into the excited state, but because there are photons at both of these frequencies a quantum mechanical interference takes place in the electron excitation resulting in an absence of absorption. This is manifested by the presence of a bright line in the transmission spectrum or a dark line in the fluorescence spectrum. In a frequency reference, laser light is used to create the two incident light fields. The frequencies of the two fields are varied while monitoring the transmitted power. When both fields are in tune with the atomic resonances there will be a detectable increase in the signal due to decreased absorption from the CPT phenomenon. Therefore, the reference oscillator used to modulate the laser frequency can then be locked to the hyperfine frequency, which provides a frequency reference.[1]

For the CPT frequency reference in this paper, the incident radiation is provided by a current-modulated VCSEL. The temperature of the system is set above 50 °C in order to increase the optical density of the Rb vapor,[4] and the laser is

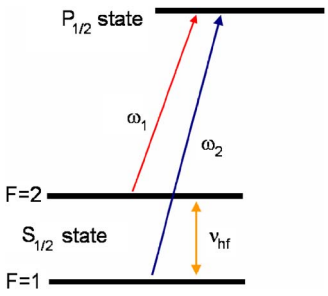

FIG. 1. (Color online) The three-level model describing the atomic resonance of Rb used to create the CPT phenomenon.

[a]Electronic mail: clong1@vcsel.micro.uiuc.edu.
[b]Electronic mail: choquett@uiuc.edu.

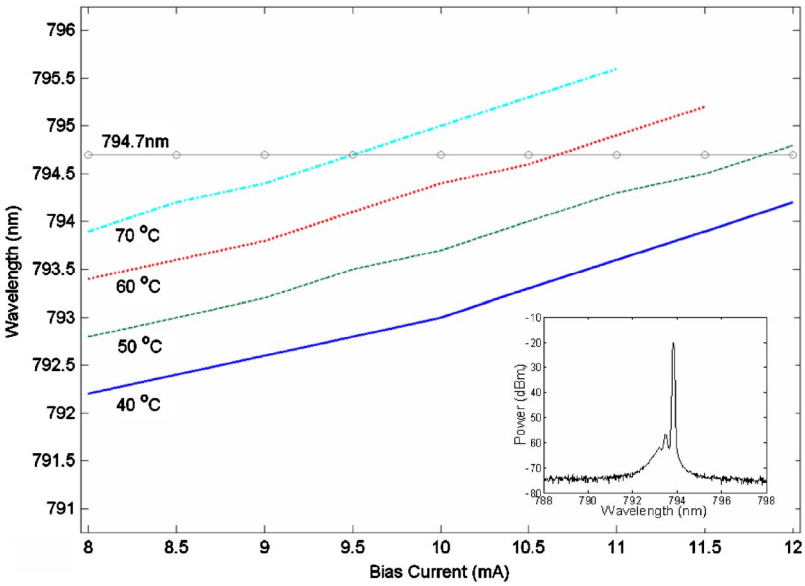

FIG. 2. (Color online) The peak wavelength of the lasing mode at various bias currents and temperatures. Inset: typical lasing spectra at 40 °C and $1.2I_{th}$.

tuned to a wavelength of 794.7 nm by adjusting its bias current. The laser is then modulated by adding a small ac current through the device.[8,9] The ac modulates the index of refraction through the free-carrier plasma effect, causing different modes to become resonant within the laser cavity and therefore providing frequency modulation (FM) to the output signal. The laser modulation thus creates a series of frequency sidebands whose amplitudes are set by the Bessel functions.[8] Thus, the operation principle is when the VCSEL is frequency modulated at one half of the hyperfine frequency, the two first-order sidebands are resonant with the Rb atomic transitions.

Direct modulation of the laser has the potential drawback of also affecting the gain within the laser and producing residual, undesirable, intensity modulation (IM). This IM effectively adds to the noise in the optical fields and asymmetries in the FM spectrum (i.e., unequal sidebands).[8] When the CPT system is pumped with asymmetric fields, there are two undesired effects. The first is a light shift due to unequal displacement of the ground states from an ac Stark effect.[10] The second is a distortion of the dark line measurement due to unequal pumping of the two transitions.[11] Therefore, operation of the VCSEL with symmetric modulation sidebands should lead to better performance of the frequency reference.

III. EXPERIMENT

To characterize VCSELs for the CPT reference, measurements of the light-current (*LI*) response, spectral mode properties, and relative intensity noise[12] (RIN) spectra are taken. These measurements are repeated at different wafer temperatures to understand how the static and dynamic properties of the VCSEL change when operated at elevated temperatures. The VCSEL modulation response is also analyzed with respect to the CPT system performance to identify parameters important for stability of the frequency reference. VCSELs generically have a threshold current and slope efficiency that are temperature dependent.[13] At sufficiently high ambient temperatures, VCSELs will produce less power until they finally cease to lase, which occurs at approximately 70 °C for the devices studied here. Figure 2 shows the peak output wavelength variation for different currents and temperature biases. From this plot, we can choose the proper set points to bias the laser and produce an output that is resonant with the Rb vapor. Also shown in Fig. 2 is a typical lasing spectrum, indicating the VCSELs operate in a single transverse mode with greater than 30 dB side mode suppression ratio.

Temperature effects could also be seen in the noise spectra of the devices. Spontaneous generation and absorption events occur within the laser cavity and produce laser RIN. Figure 3 shows a typical RIN spectrum which exhibits a peak at the laser relaxation oscillation frequency, and the variation of the square of the laser relaxation oscillation frequency f_R with output power is also shown. The relaxation oscillation frequency is a key factor in the modulation response of a laser; under moderate output powers and damping, it is directly proportional to the modulation bandwidth of the laser. For each temperature, the RIN data are measured at the same bias currents. As the wafer temperature increases, we find that f_R decreases due to decreased output power of the VCSELs at a given bias current. This is predicted by RIN theory,[14] which shows f_R^2 varies proportionally with photon number density N_P. This trend is important for understanding the CPT system response.

The output of a VCSEL undergoing FM is shown in the laser spectra of Fig. 4(a), where the carrier (J_0), first-order (J_1), and second-order (J_2) sidebands are indicated. The VCSEL is operated at room temperature and biased at approximately $2I_{th}$. When the laser is biased at lower currents or higher temperatures (not shown), it is found that the J_1 sidebands become more symmetric.

IV. ANALYSIS

The ideal VCSEL for a CPT system is one that has no IM, produces symmetric sidebands under modulation, and has low noise. In order to understand how these properties are interrelated, we first examine the small signal transfer functions of both IM and FM. Next, we show how these

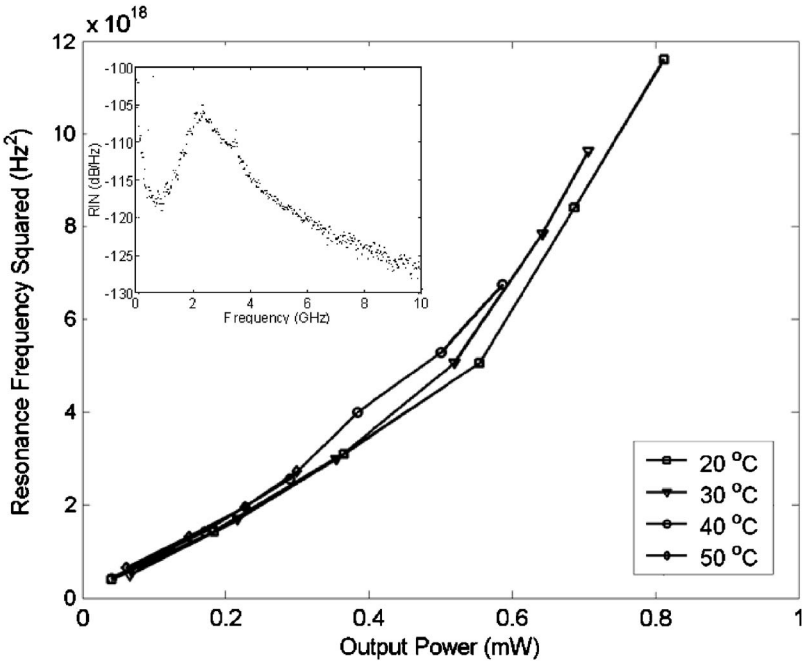

FIG. 3. Variation of the resonance frequency of a VCSEL with output power and temperature. Inset: typical RIN spectrum at 40 °C and $1.2I_{th}$.

parameters affect the output spectrum of the modulated fields in order to interpret the measured response of the VCSEL in the CPT system.

The IM response of a directly modulated laser is proportional to the modulation transfer function $H(\omega)$ as[14]

$$\frac{P}{I} \propto H(\omega) = \frac{\omega_R^2}{\omega_R^2 - \omega^2 + j\omega\gamma}. \tag{1}$$

In Eq. (1), P is the output power modulated at frequency ω and I is the modulation current. The ω_R term is the relaxation oscillation frequency expressed in radians per second and γ is the damping factor.

The FM response follows the modulation transfer function, but with an additional zero in the transfer equation at γ_{PP},[14]

$$\frac{\nu_1}{I_1} \propto (\gamma_{PP} + j\omega)H(\omega). \tag{2}$$

In Eq. (2), ν_1 is the modulated optical frequency and γ_{PP} is related to the effective photon lifetime; it contributes to both the damping and the relaxation oscillation frequency of the laser. Above threshold, it is approximated as proportional to N_P,

$$\gamma_{PP} \approx \Gamma v_g a_P N_P. \tag{3}$$

Equation (3) introduces the differential gain with respect to photon density a_P the optical confinement factor Γ, and the group velocity of light v_g.

Equations (1) and (2) are for small-signal modulation deliberately introduced into the system through current injection, but spontaneously generated photons are also affected by the cavity dynamics of the laser and have a frequency response given by[4]

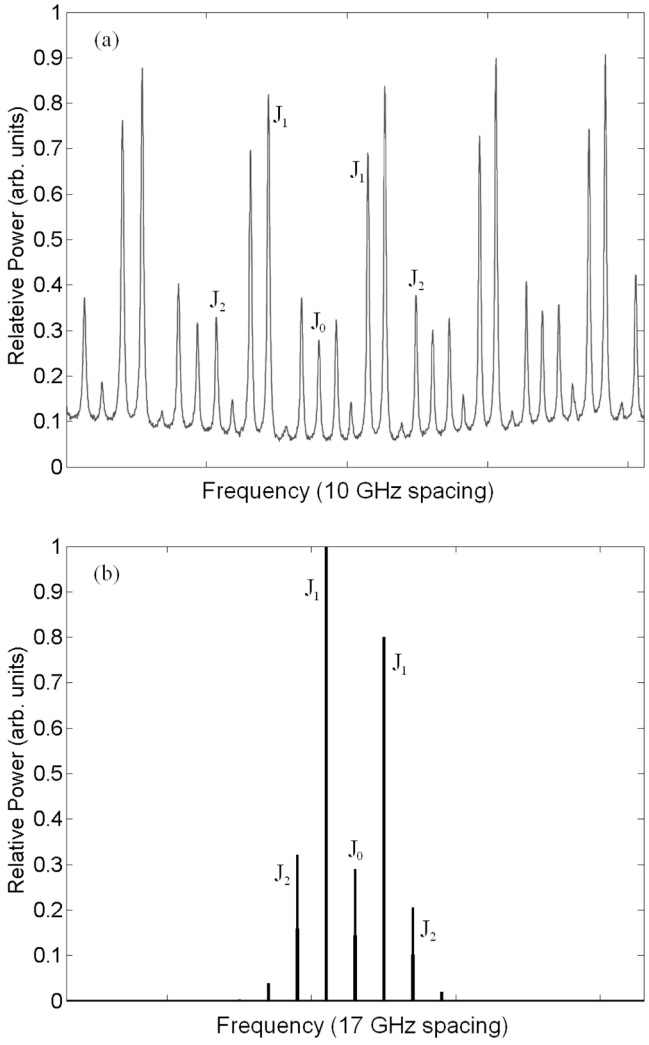

FIG. 4. (Color online) (a) Measured FM response of a VCSEL biased at $2.0I_{th}$ and room temperature with a modulation power of −16.5 dBm. Carrier (J_0), first-order (J_1), and second-order (J_2) sidebands are as shown. (b) Simulation result of VCSEL biased under the same conditions. Simulation parameters are listed in Table I.

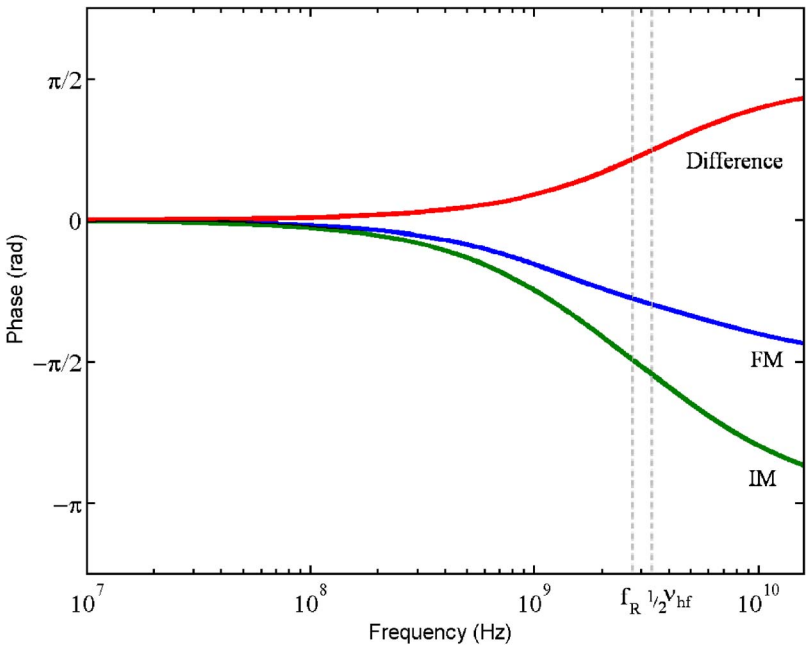

FIG. 5. (Color online) The IM and FM phase response of a VCSEL at room temperature and $2.0I_{th}$ with the resonance frequency and modulation frequency indicated. Simulation parameters are listed in Table I.

$$\mathrm{RIN} = \frac{a_1 + a_2\omega^2}{(\omega_R^2 - \omega^2) + \omega^2\gamma^2}\ (\mathrm{dB/Hz}). \tag{4}$$

By using a_1 and a_2 as fitting parameters in Eq. (4), we can extract the damping factor and resonance frequency of a laser from its RIN spectrum, such as shown in Fig. 3.

Plots of the phase for the modulation transfer functions are given in Fig. 5. The IM phase response is plotted using Eq. (1) with values for γ and ω_R taken from a measured RIN spectrum. In order to plot the FM phase response using Eq. (2), we also need the value of γ_{PP}.[15] According to theory,[14] γ_{PP} is only a fraction of the total laser damping, so we set it to be one-half of the total damping as a first order approach.

From the phase and magnitude of the modulation response, we can see how they affect the output power spectra of a directly modulated laser. As previous work has shown,[8,9] the asymmetry in the modulation sidebands is a result of the residual IM that accompanies a directly modulated laser. For the model presented in Ref. 9, a diode laser is modulated with a sinusoidal source at frequency f_m and produces a modulated signal, $m(t)$, described by

$$m(t) = \sqrt{1 + m\sin(2\pi f_m t + \varphi_{\mathrm{IM}})}\exp[j\beta\cos(2\pi f_m t + \varphi_{\mathrm{FM}})]. \tag{5}$$

In Eq. (5), m is the IM factor, given by the ratio of the modulated power to that of the cw power, and β is the FM index, given by the ratio of the peak frequency deviation to the modulation frequency. The phase terms φ_{IM} and φ_{FM} result from the arguments of the modulation transfer functions discussed above in Eqs. (1) and (2). The power spectrum of a laser undergoing direct modulation can be obtained from a Fourier transform of Eq. (5).

The parameters in Eq. (5) that we can modify are β, m, and φ. The FM index β determines the relative power in each band and is typically set to minimize the light shift of the system,[10] leaving m and φ as potential operation parameters. For the case of $m=0$, the laser experiences pure FM, that is, frequency variation without intensity modulation. Under this condition, the laser always produces an output with equal sidebands. We can approach this ideal situation by modulating the laser above its relaxation oscillation frequency, where m quickly decreases due to a double pole in the IM transfer function. We also note that the laser slope efficiency decreases at higher temperatures,[13] which can also help to minimize m.

We can also vary the output power spectrum through the two phase terms. Power spectrum analysis of Eq. (5) shows that when the difference between φ_{FM} and φ_{IM} equals odd multiples of $\pi/2$, the output signal will have equal power in the J_1 sidebands. The laser will begin to experience this condition when it is modulated at a frequency that is significantly greater than γ_{PP}. This analysis supports experimental observation in the system response. When the output power is decreased through lower bias current or higher temperature, γ_{PP} also decreases due to its proportionality with photon number density. By lowering the value of γ_{PP}, it increases the phase of the FM response at the modulation frequency and pushes the phase difference between φ_{FM} and φ_{IM} closer to $\pi/2$.

Using data obtained from the phase plot in Fig. 5, we can calculate the normalized power spectra of the device shown in Fig. 4(b). The J_1 sidebands are asymmetric as expected. Using the parameters listed in Table I, we find that by

TABLE I. Parameters used to calculate the phase of the IM and FM responses and the modulation power spectrum.

Parameter	Value
γ	6.8×10^9/s
γ_{PP}	3.4×10^9/s
f_R	2.81×10^9 Hz
Modulation frequency	3.417×10^9 Hz
β	1.825
m	0.29

reducing γ_{PP} and f_R, we can obtain more symmetric J_1 sidebands, which will lead to improved performance of VCSELs in CPT frequency references.

V. CONCLUSION

In this paper, we examine the optical properties of a VCSEL to characterize its performance within a CPT-based frequency reference. The VCSEL output power, laser wavelength, and single transverse mode are found to be appropriate for this application. The performance of the frequency reference is directly related to the power in the two radiation fields of the frequency modulated VCSEL that produce the CPT phenomenon. The VCSEL sideband asymmetry results from the difference in phase between the IM and FM responses. Consequently, an optimized VCSEL for a CPT frequency reference will be one designed to have a low relaxation oscillation frequency. Previous work has cited a minimum bandwidth that is necessary to ensure efficient power in the modulation sidebands;[16] the work presented here suggests that there is also a maximum desirable bandwidth. When the VCSEL is modulated at one-half of the hyperfine splitting frequency, this modulation should be well above a lower relaxation oscillation frequency of the laser to produce lower residual IM and a phase difference between the FM and IM responses that approaches $\pi/2$. Either of these conditions will ensure symmetry of the first-order sidebands which will lead to better CPT performance. It is interesting to note that a high value of relaxation oscillation frequency is desirable in data communication VCSEL sources. In summary, the optical properties of VCSELs can be suitably designed to produce the appropriate single-mode output at a specific wavelength with low noise and low relaxation oscillation frequency. Using VCSELs in a coherent population, trapping-based frequency reference will enable new applications that require accurate timing or position determination.

ACKNOWLEDGMENTS

The authors acknowledge the support and advice of Kernco, Inc.

[1] J. Vanier, M. W. Levine, D. Janssen, and M. J. Delaney, IEEE Trans. Instrum. Meas. **52**, 258 (2003).
[2] S. Knappe, V. Shah, P. D. D. Schwindt, L. Hollberg, J. Kitching, L. Liew and J. Moreland, Appl. Phys. Lett. **85**, 1460 (2004).
[3] R. Lutwak, D. Emmons, T. English, W. Riley, A. Duwel, M. Varghese, D. K. Serkland, and G. M. Peake, Proceedings of the 34th Annual Precise Time and Time Interval (PTTI) Systems Applications Meeting, San Diego, CA, 2003 (unpublished), p. 467.
[4] J. Vanier, Appl. Phys. B: Lasers Opt. **81**, 421 (2005).
[5] K. D. Choquette and K. M. Geib, in *Vertical Cavity Surface Emitting Lasers*, edited by C. Wilmsen, H. Temkin, and L. Coldren (Cambridge University Press, Cambridge, UK, 1999), p. 193.
[6] H. P. Zappe, Proceedings of the 31st Annual Precise Time and Time Interval (PTTI) Meeting, Dana Point, CA, 1999 (unpublished), p. 589.
[7] C. Affolderbach, A. Nagel, S. Knappe, C. Jung, D. Wiedenmann, and R. Wynands, Appl. Phys. B: Lasers Opt. **70**, 407 (2000).
[8] S. Kobayashi, Y. Yamamoto, M. Ito, and T. Kimura, IEEE J. Quantum Electron. **QE-18**, 582 (1982).
[9] H. Olesen and G. Jacobsen, IEEE J. Quantum Electron. **QE-18**, 2069 (1982).
[10] F. Levi, A. Godone, and J. Vanier, IEEE Trans. Ultrason. Ferroelectr. Freq. Control **47**, 466 (2000).
[11] F. Levi, A. Godone, J. Vanier, S. Micalizio, and G. Modugno, Eur. Phys. J. D **12**, 53 (2000).
[12] Y. Yamamoto, IEEE J. Quantum Electron. **QE-19**, 34 (1983).
[13] B. Tell, K. F. Brown-Goebeler, R. E. Leibenguth, F. M. Baez, and Y. H. Lee, Appl. Phys. Lett. **60**, 683 (1992).
[14] L. A. Coldren and S. W. Corzine, *Diode Lasers and Photonic Integrated Circuits* (Wiley, New York, 1995).
[15] R. Shimpe, J. E. Bowers, and T. L. Koch, Electron. Lett. **22**, 453 (1986).
[16] D. K. Serkland, G. M. Peake, K. M. Geib, R. Lutwak, R. M. Garvey, M. Varghese, and M. Mescher, Proc. SPIE **6132**, 66 (2006).